Photocatalysis

DOI: 10.1002/ange.201311209

Pigment–Acceptor–Catalyst Triads for Photochemical Hydrogen Evolution**

*Kyoji Kitamoto and Ken Sakai**

Abstract: *In order to solve the problems of global warming and shortage of fossil fuels, researchers have been endeavoring to achieve artificial photosynthesis: splitting water into H_2 and O_2 under solar light illumination. Our group has recently invented a unique system that drives photoinduced water reduction through "Z-scheme" photosynthetic pathways. Nevertheless, that system still suffered from a low turnover number (TON) of the photocatalytic cycle (TON = 4.1). We have now found and describe herein a new methodology to make significant improvements in the TON, up to around TON = 14–27. For the new model systems reported herein, the quantum efficiency of the second photoinduced step in the Z-scheme photosynthesis is dramatically improved by introducing multiviologen tethers to temporarily collect the high-energy electron generated in the first photoinduced step. These are unique examples of "pigment–acceptor–catalyst triads", which demonstrate a new effective type of artificial photosynthesis.*

Due to the shortage of fossil fuels, solar-driven water splitting into H_2 and O_2 has been extensively studied for many years.[1,2] Nature invented two light-harvesting units, that is, photosystem II (PSII) and photosystem I (PSI), which are rationally coupled with water oxidation and hydride (H^-) addition reactions, respectively. The latter corresponds to storage of reducing equivalents in the form of an organic molecule (the reduced form of nicotinamide adenine dinucleotide phosphate; NADPH) and is conceptually equivalent to the production of H_2 from H^- and H^+. Therefore, artificial photosynthesis systems driving both photoinduced water oxidation and reduction are important targets of research (Scheme 1).

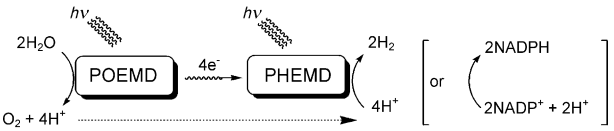

Scheme 1. Artificial photosynthesis based on a photo-oxygen-evolving molecular device (POEMD) and a photo-hydrogen-evolving molecular device (PHEMD).

Up to now, considerable efforts have been made to develop PHEMDs consisting of a $Ru(bpy)_3^{2+}$-type photosensitizer (bpy: 2,2′-bipyridine) and a Pt^{II}-based molecular water reduction catalyst; these efforts resulted in our previous reports on a series of RuPt-based PHEMDs,[3] such as "$RuPt^{2+}$" (Scheme 2). Simple mononuclear Pt^{II} complexes

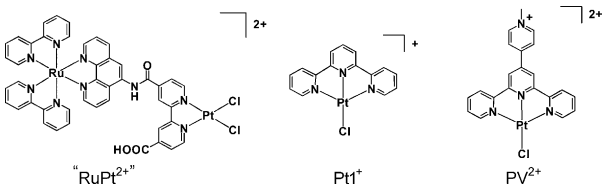

Scheme 2. Some examples of Pt^{II}-based PHEMDs.

($Pt1^+$ from ref. [4] and PV^{2+} from ref. [5]; Scheme 2) have also been realized to serve as PHEMDs. Although these complexes are considered as important examples of PHEMDs, the turnover numbers (TONs) of the photocatalysts (TON = 3–5) were rather low compared to those reported for the cobalt-based supramolecular systems studied by Artero and coworkers.[6]

One of our recent studies provided an important indication concerning the improvement of the TON.[5b] The study showed that PV^{2+} (Scheme 2) affords the doubly reduced species PV^0 based on two successive photoinduced processes, which we defined as "Z-scheme photosynthesis" (PV^{2+} + ethylenediaminetetraacetate (EDTA) + $h\nu \rightarrow PV^{+\bullet} + EDTA^+$; $PV^{+\bullet} + EDTA + h\nu \rightarrow PV^0 + EDTA^+$; $PV^0 + 2H^+ \rightarrow PV^{2+} + H_2$; Z-scheme photosynthesis A in Scheme 3). In this photolysis, a π-radical-like colored intermediate, possessing broad absorption bands in the visible to NIR region, is generated first and its photoexcited state (that is, $PtL^{-\bullet}$*) must

[*] K. Kitamoto, Prof. K. Sakai
Department of Chemistry, Faculty of Sciences, Kyushu University
Hakozaki 6-10-1, Higashi-ku, Fukuoka, 812-8581 (Japan)
and
International Institute for Carbon-Neutral Energy Research (WPI-I2CNER), Kyushu University (Japan)
E-mail: ksakai@chem.kyushu-univ.jp
Prof. K. Sakai
Center for Molecular Systems (CMS), Kyushu University (Japan)

[**] This work was partly supported by a Grant-in-Aid for Scientific Research (B) (grant no. 24350029), a Grant-in-Aid for Scientific Research on Innovative Areas "Coordination Programming" (No. 2107) (grant no. 24108732), and a Grant-in-Aid for Scientific Research on Innovative Areas "Artificial Photosynthesis" (No. 2406) (grant no. 24107004) from the Ministry of Education, Culture, Sports, Science, and Technology (MEXT) of Japan. This was further supported by the International Institute for Carbon Neutral Energy Research (WPI-I2CNER), sponsored by the World Premier International Research Center Initiative (WPI), MEXT (Japan). K.K. acknowledges Research Fellowships of the Japan Society for the Promotion of Science for Young Scientists.

Supporting information for this article is available on the WWW under http://dx.doi.org/10.1002/anie.201311209.

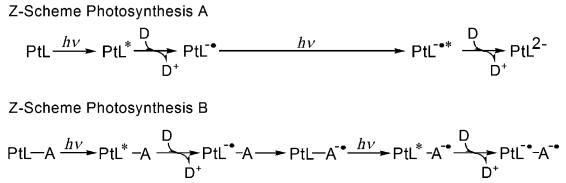

Scheme 3. Strategy to improve the efficiency in the second photo-induced electron-transfer step. A is an acceptor, D is EDTA (a donor), and L (the ligand) corresponds to bpy, 2,2′:6′,2″-terpyridine (tpy), etc.

be further reductively quenched by EDTA at higher-energy excited states prior to the internal conversion leading to the lower-energy excited states, which are correlated with the visible to NIR absorptions of the $PtL^{-\bullet}$ species. We now suppose that such deactivation could be substantially suppressed by tethering of electron reservoir moieties because the reduced form of the PtL moiety ($PtL^{-\bullet}$) can be immediately converted into its original nonreduced form (PtL) by simple intramolecular electron transfer ($PtL^{-\bullet}$–A → PtL–$A^{-\bullet}$; Z-scheme photosynthesis B in Scheme 3; Figure S1 in the Supporting Information). Herein, we report on the photochemical H_2-evolving activities of three $[PtCl_2(bpy)]$ derivatives tethered to multiviologen moieties, PtL–A_n (n: 2 or 4), together with those of the related systems (Scheme 4). This study reveals that these multiviologen derivatives indeed exhibit much higher TONs (14–27) in visible-light-induced water reduction in the presence of EDTA.

Although the molar absorptivities of $[PtCl_2(4,4'\text{-MV2})]^{4+}$, $[PtCl_2(4,4'\text{-MV4})]^{8+}$, and $[PtCl_2(5,5'\text{-MV4})]^{8+}$ in the visible region are not sufficiently high, their lowest energy band, corresponding to the metal-to-ligand charge transfer (MLCT) transitions derived from the $[PtCl_2(bpy)]$ chromophore[7,8] ($\lambda_{max} = 386$–388 nm, $\varepsilon = 2300$–$3800\,M^{-1}cm^{-1}$), has a tail up to around 500 nm (Figure S2). This feature allows them to generate photoexcited states upon visible-light illumination. The concentration dependences of absorbance at several wavelengths all satisfy Beer's law, which precludes the possibility of them to form a stacked dimer in the ground state under these experimental conditions (Figure S3). On the other hand, these triads exhibit emissions in methanol/ethanol/*N*,*N*-dimethylformamide (MED; 4:4:1) under frozen glass conditions (at 77 K; Figure S5 and Table S3). Based on the relatively large Stokes shifts (approximately 100 nm) and long-lived characters (7.37–9.13 μs; Figure S7), these emissions are considered to arise from the triplet excited (^{3}MLCT) states.

The absorption and emission properties of $[PtCl_2(4,4'\text{-MP1})]^+$, $[PtCl_2(4,4'\text{-MP2})]^{2+}$, and $[PtCl_2(5,5'\text{-MP2})]^{2+}$ (Figures S4, S6, and S8) are quite similar to those of the corresponding MV2/MV4 derivatives (Figures S2, S5, and S7). However, intramolecular oxidative quenching of these MP1/MP2 derivatives with their methylpyridinium residues is not favored due to the large cathodic shifts in the reduction potentials of these residues (−1.67 to −1.75 V vs. Fc/Fc^+; Fc: ferrocene; Table S6) in comparison with those of the MV2/MV4 residues (−0.81 to −0.89 V vs. Fc/Fc^+; Table S5). This reveals that the methylpyridinium moieties in the **MP1**/**MP2** derivatives can simply serve as positive groups to let them

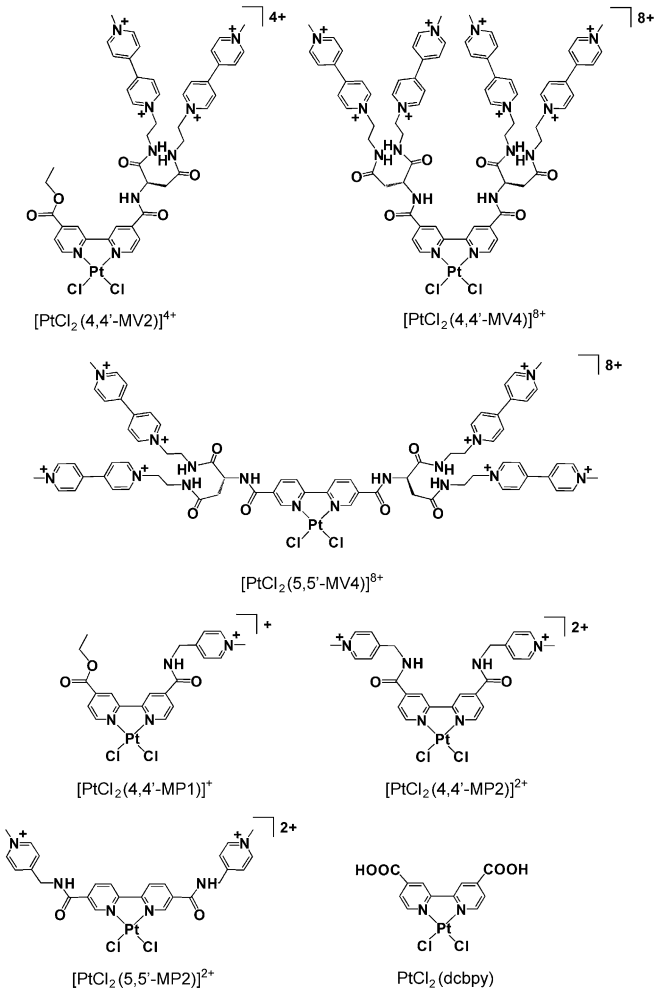

Scheme 4. New PHEMDs (PtL–A_n derivatives) together with controls. MV: multiviologen; MP: methylpyridinium; dcbpy: 4,4′-dicarboxy-2,2′-bipyridine.

form an ion pair with the dianionic form of EDTA (YH_2^{2-}, if EDTA is YH_4; 93% abundance at pH 5.0).[4]

Figure 1 shows the photochemical hydrogen-evolution characteristics of these triads when they are photolyzed in the presence of EDTA at pH 5.0. It can be seen that the MP1/MP2 derivatives also serve as PHEMDs, although their activities are much lower than those of the MV2/MV4 derivatives (Figure S9a–c). On the other hand, the control with no positive charges on the ligand, that is, $[PtCl_2(dcbpy)]$, does not at all show activity as a PHEMD (Figure S9d), even in the presence of free methylviologen (MV^{2+}; Figure S10 and Table S4). These results reveal that positively charged moieties tethered to the bpy ligands are essential for the generation of electron-transferred products that lead to H_2 evolution from water. As demonstrated in our previous studies,[3–5] these behaviors are obviously correlated with ion-pair adduct formation [Eq. (1)].

It must also be noted here that such highly charged multiviologen-tethered Ru and Pt complexes do ion-pair with counteranions (PF_6^-, Cl^-, etc.) in aqueous media.[8,9] The initial photoproduct during the photolysis of the MV2/MV4/

$$\mathrm{PHEMD}^{n+} + \mathrm{YH_2}^{2-} \rightleftharpoons [\mathrm{PHEMD\text{-}YH_2}]^{(n-2)+} \xrightarrow{h\nu} [\mathrm{PHEMD}^{*}\text{-}\mathrm{YH_2}]^{(n-2)+} \xrightarrow{\text{reductive quenching}} [\mathrm{PHEMD}^{-}]^{(n-1)+} + \mathrm{YH_2}^{-} \quad (1)$$

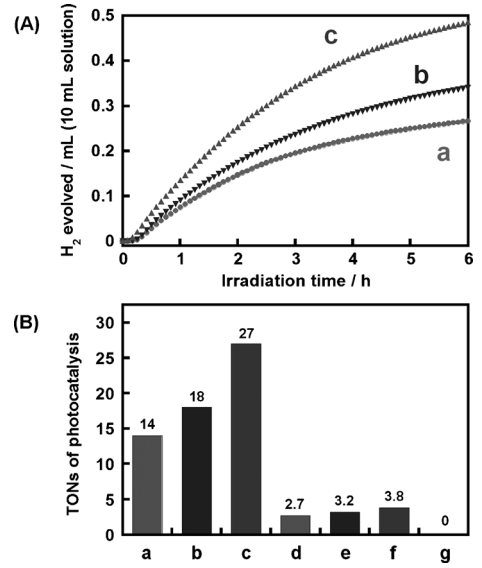

Figure 1. A) Visible-light-induced H_2 production (>400 nm) from an aqueous acetate buffer solution (0.03 M CH_3COOH and 0.07 M CH_3COONa; pH 5.0, 10 mL; at 20 °C under Ar) containing 0.1 M NaCl and 30 mM EDTA in the presence of 0.1 mM a) $[PtCl_2(4,4'\text{-MV2})](PF_6)_4\cdot 3H_2O$, b) $[PtCl_2(4,4'\text{-MV4})](PF_6)_8\cdot 4H_2O$, and c) $[PtCl_2(5,5'\text{-MV4})](PF_6)_8\cdot 5H_2O$. B) The turnover numbers of a) $[PtCl_2(4,4'\text{-MV2})](PF_6)_4\cdot 3H_2O$, b) $[PtCl_2(4,4'\text{-MV4})](PF_6)_8\cdot 4H_2O$, c) $[PtCl_2(5,5'\text{-MV4})](PF_6)_8\cdot 5H_2O$, d) $[PtCl_2(4,4'\text{-MP1})](PF_6)\cdot 2H_2O$, e) $[PtCl_2(4,4'\text{-MP2})](PF_6)_2\cdot 3H_2O$, f) $[PtCl_2(5,5'\text{-MP2})](PF_6)_2\cdot 5H_2O$, and g) $[PtCl_2(dcbpy)]$.

MP1/MP2 derivatives is likely to involve $\{Pt^{II}Cl_2(bpy^{-\bullet})\}$, which must occur as a result of reductive quenching of $\{PtCl_2(bpy)^*\}$ (^{3}MLCT state, formally described as $\{Pt^{III}Cl_2(bpy^{-\bullet})\}$) only within the above ion-pair adducts because of the nonemissive (that is, short-lived) characters of them under these conditions.

Table 1 shows the photo-hydrogen-evolving activities of the Pt^{II}-based PHEMDs developed so far in our group. The multiviologen-tethered PHEMDs exhibit much higher TONs than the Pt^{II}-based derivatives reported to date. As noted above, the $[Pt^{II}Cl_2(bpy)]$-based chromophore can be rapidly regenerated after formation of $\{Pt^{II}Cl_2(bpy^{-\bullet})\}$ by forming $\{Pt^{II}Cl_2(bpy)\text{–}(A)_{n-1}(A^{-\bullet})\}$. Otherwise, even oxidative quenching of $\{PtCl_2(bpy)^*\}$ by a viologen tether occurs to afford $\{Pt^{III}Cl_2(bpy)\text{–}(A)_{n-1}(A^{-\bullet})\}$ followed by rapid reduction of the Pt^{III} center by EDTA to yield the same photoproduct. It also seems possible that these two quenching processes compete with one another, as demonstrated for "$RuPt^{2+}$".[3f] Thus, the light-harvesting centers of the MV2/MV4 derivatives possess an important "regenerable character", which is not available for the MP1/MP2 derivatives or

Table 1: Comparison of the catalytic performances of PHEMDs.[a]

Entry	System	Irradiation time [h]	TON	Ref.
1	"$RuPt^{2+}$"	10	4.8	[3a]
2	$Pt1^+$	7	3	[4]
3	PV^{2+}	12	4.1	[5]
4[b]	$[PtCl_2(4,4'\text{-MV2})]^{4+}$	6	12	this work
		12	14	
5[b]	$[PtCl_2(4,4'\text{-MV4})]^{8+}$	6	15	this work
		12	18	
6[b]	$[PtCl_2(5,5'\text{-MV4})]^{8+}$	6	22	this work
		12	27	
7[b]	$[PtCl_2(4,4'\text{-MP1})]^{+}$	6	2.7	this work
8[b]	$[PtCl_2(4,4'\text{-MP2})]^{2+}$	6	3.2	this work
9[b]	$[PtCl_2(5,5'\text{-MP2})]^{2+}$	6	3.8	this work
10[b]	$PtCl_2(dcbpy)$	2	0	this work

[a] Photochemical H_2 production from an aqueous acetate buffer solution (pH 5.0, 10 mL) containing 30 mM EDTA. [b] Reaction performed in the presence of 0.1 M NaCl to minimize the concentration of hydrolysis products.

PV^{2+}.[5b] As previously demonstrated for PV^{2+},[5b] the addition of one equivalent of *cis*-$[PtCl_2(NH_3)_2]$ to one of the systems (for example, $[PtCl_2(4,4'\text{-MV4})]^{8+}$) was found to double the initial H_2 evolution rate (Figure S30), which reveals that intermolecular H_2 evolution paths can also take place.

The electrochemical properties of the triads (Figure S11 and Table S5) allow us to discuss the driving force of intramolecular electron transfer in the reductively quenched product $\{Pt^{II}Cl_2(bpy^{-\bullet})\text{–}(A)_n\}$, which affords the photoproduct $\{Pt^{II}Cl_2(bpy)\text{–}(A)_{n-1}(A^{-\bullet})\}$. For all of the triads, no electrochemical communication is obvious for the viologen-based redox couples (Figure S11). On this basis, the free-energy change with regard to the intramolecular electron transfer (ΔG_{IET}) can be estimated from the difference in potential for the first reduction at viologen and that at bpy, that is, $E_{1/2}(A/A^{-\bullet})$ and $E_{1/2}(bpy/bpy^{-\bullet})$, respectively. The values are estimated as $\Delta G_{IET} = -0.48$, -0.54, and -0.29 eV for $[PtCl_2(4,4'\text{-MV2})]^{4+}$, $[PtCl_2(4,4'\text{-MV4})]^{8+}$, and $[PtCl_2(5,5'\text{-MV4})]^{8+}$, respectively. These values reflect the exceptionally positive-shifted $E_{1/2}(bpy/bpy^{-\bullet})$ value for $[PtCl_2(5,5'\text{-MV4})]^{8+}$ (-1.18 V vs. Fc/Fc^+; Table S5). This indicates that the reduction potential of the ^{3}MLCT state, defined below in Equation (2), in which E_{em} denotes the emission energy of the triplet, is highest for $[PtCl_2(5,5'\text{-MV4})]^{8+}$.

$$E_{1/2}(PtCl_2(bpy)^*/PtCl_2(bpy^{-\bullet})) = E_{em} + E_{1/2}(bpy/bpy^{-\bullet}) \quad (2)$$

Consequently, the driving force for the reductive quenching of the triplet by EDTA must be largest for $[PtCl_2(5,5'\text{-MV4})]^{8+}$, which can be well correlated with its highest activity as a PHEMD.

On the other hand, the $E_{1/2}(A/A^{-\bullet})$ value for the MP1/MP2 derivatives shows a large cathodic shift (Table S6). Therefore, the intramolecular electron transfer from $\{Pt^{II}Cl_2(bpy^{-\bullet})\text{–}(A)_n\}$ to $\{Pt^{II}Cl_2(bpy)\text{–}(A)_{n-1}(A^{-\bullet})\}$ is a highly uphill process in each case, with the ΔG_{IET} values estimated as 0.47, 0.44, and 0.49 eV for $[PtCl_2(4,4'\text{-MP1})]^+$, $[PtCl_2(4,4'\text{-MP2})]^{2+}$, and $[PtCl_2(5,5'\text{-MP2})]^{2+}$, respectively (Figure S12 and

Table S6), which indicates that the formation of $\{Pt^{II}Cl_2(bpy)-(A)_{n-1}(A^{-\bullet})\}$ is not thermodynamically favored for these systems. The $E_{1/2}(bpy/bpy^{-\bullet})$ value is most positive shifted for $[PtCl_2(5,5'\text{-MP2})]^{2+}$ (−1.18 V vs. Fc/Fc^+; Table S6). For either MV2/MV4 or MP1/MP2 derivatives, the 5,5′-substituted derivative shows the highest activity as a PHEMD among each series. Therefore, it seems quite likely that the driving force for the reductive quenching of the ^{3}MLCT state by EDTA governs the net photocatalytic efficiency.

Next, we pay attention to the number of electrons stored over the multiviologen tethers within each framework. It is expected that more than one reducing equivalent can be transferred to the multiviologen tethers as a result of successive reductive quenching reactions. As a typical example, the absorption spectral changes during the H_2 evolution driven by $[PtCl_2(4,4'\text{-MV4})]^{8+}$ are shown in Figure 2 A. This is

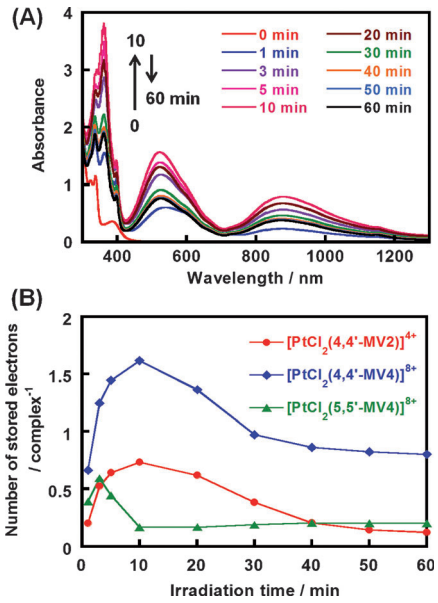

Figure 2. A) Spectral changes during the photolysis of an aqueous acetate buffer solution (pH 5.0; at 20 °C under Ar) containing 0.1 mM $[PtCl_2(4,4'\text{-MV4})]^{8+}$, 0.1 M NaCl, and 30 mM EDTA. B) Changes in the total number of electrons stored within a framework during photolysis.

similar to the charge-storage behavior previously observed for photoinduced H_2 evolution driven by a combination of $[Ru(bpy)_3]^{2+}$ and $[PtCl_2(MV_n)]$ ($n=2$, 4, or 6; MV_n denotes 5,5′-substituted-bpy ligands tethered to 2, 4, and 6 viologen units) in the presence of EDTA,[8] for which oxidative quenching of $[Ru(bpy)_3]^{2+*}$ by $[PtCl_2(MV_n)]$ was assumed to be the major electron-transfer event. In other words, we were unware of the activity of $[PtCl_2(MV_n)]$ as a PHEMD in that study. As previously described,[8] the 900 nm band corresponds to a diradical species, which occurs as a consequence of specific stabilization of a stacked dimer $(MV^{+\bullet})_2$ within the same residue. The spectral features of this diradical species are quite consistent with those previously reported by Lee et al.[10] and also with those previously observed for $[PtCl_2(MV_n)]$.[8] On the other hand, the 602 nm band corresponds to a monoradical species. Based on our published methods,[8] deconvolution was carried out to determine the relative abundances of the $MV^{+\bullet}$ and $(MV^{+\bullet})_2$ species at each irradiation time (Table S9). Consequently, the time course of the number of electrons stored within a framework can be viewed for all of these triads, as depicted in Figure 2 B. For both $[PtCl_2(4,4'\text{-MV2})]^{4+}$ and $[PtCl_2(4,4'\text{-MV4})]^{8+}$, the total number of electrons shows a maximum at around 10 min and gradually decreases as the reaction proceeds, which suggests that an induction period is spent and then a stationary state is established, during which the formation and consumption of the radical species are balanced in rate, as previously observed.[8] These results are also consistent with the induction periods observed in the H_2 evolution profiles of these triads in Figure 1 A (see also the Supporting Information). The behavior of $[PtCl_2(5,5'\text{-MV4})]^{8+}$ is essentially similar to those of the 4,4′-substituted derivatives, but the maximum appears much earlier at around 3 min, which must be viewed as related to the largest driving force of reductive quenching being estimated for this system (see above). The apparent dimerization constants (K_D) are in the range of 10^3–$10^5\,M^{-1}$ (Tables S8–S10) and are much larger than the K_D values reported for free MV^{2+} in aqueous media ($K_D = 550\,M^{-1}$),[10] which reveals that the present dipeptide backbone provides an extraordinary stabilization effect for the diradical species.

The dependence of the initial H_2 evolution rate on the EDTA concentration obeys Michaelis–Menten kinetics for all of these triads (Figures S19–S21). Importantly, no H_2 evolves in the absence of EDTA. This behavior is quite similar to those previously observed for most of the PHEMDs developed so far in our group.[3–5] Saturation behaviors are also seen when the PHEMD concentration is varied at a constant EDTA concentration (Figures S22–24). In the same manner, nanosecond transient absorption (TA) spectroscopy (Figure 3) shows that a photoproduct attributable to $\{Pt^{II}Cl_2(bpy)-(A)_{n-1}(A^{-\bullet})\}$ is only observable in the presence of EDTA. Moreover, for all of the triads, the yield of photoproduct monitored by TA spectroscopy exhibits saturation with regard to the variation in the EDTA concentration (Figure 3 B; Figures S25 and S26). These results strengthen our conclusion that the electron injection from the YH_2^{2-} species ion paired with the cationic PHEMD is the key to afford the initial photoproduct $\{Pt^{II}Cl_2(bpy)-(A)_{n-1}(A^{-\bullet})\}$.

Finally, in situ dynamic light scattering (DLS) measurements were carried out to ascertain the lack of colloidal platinum dispersion during the H_2 evolution photocatalyzed by these multivilogen-tethered PHEMDs. As shown in Figure 4, variations in the light-scattering intensity for all of these triads during the photolysis were negligible and the development of any exponential decay feature in the correlation functions was also negligible (Figures S27–S29). These results clearly show that the formation of colloidal platinum particles can be ruled out during the H_2 evolution photocatalyzed by these triads. For comparison, Figure 4 shows the manner in which the light-scattering intensity increases when the same amount of a well-known colloid precursor (K_2PtCl_4) is converted into colloidal platinum particles under the same experimental setup. These results clearly indicate that the photocatalytic H_2 generation driven by these multiviologen-

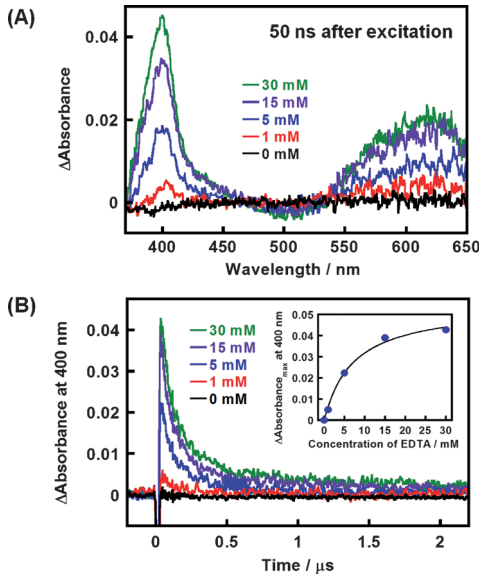

Figure 3. A) Nanosecond transient absorption spectra observed for an aqueous acetate buffer solution (pH 5.0; at room temperature under Ar) containing 0.1 mM $[PtCl_2(4,4'\text{-}MV4)]^{8+}$, 0.1 M NaCl, and EDTA at various concentrations (0–30 mM), recorded at 50 ns after laser pulse excitation at 355 nm. B) Transient traces at 400 nm, corresponding to the decay of the photoproducts. The inset shows the dependence of the maximum absorbance at 400 nm on the EDTA concentration (0–30 mM).

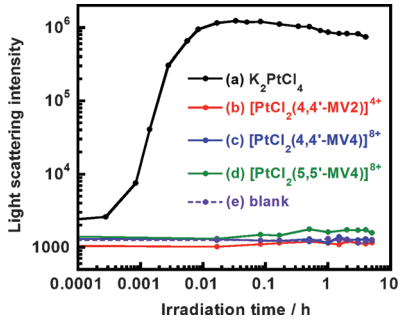

Figure 4. DLS measurements during the photolysis of an aqueous acetate buffer solution (pH 5.0; at 20°C under Ar) containing 0.1 M NaCl in the presence of a) 30 mM EDTA, 0.04 mM $[Ru(bpy)_3]Cl_2{\cdot}6H_2O$, 2 mM $[MV]Cl_2$, and 0.1 mM K_2PtCl_4, b–d) 30 mM EDTA and 0.1 mM PHEMD, and e) 30 mM EDTA (blank).

tethered PHEMDs proceeds based on "homogeneous catalysis".

In summary, we have shown that such a simple $[PtCl_2(bpy)]$-based MLCT band can be used to drive the solar water-reduction process, although the problem arising from the low absorptivity should be solved to improve the overall energy-conversion efficiency in view of more practical application purposes. We have also demonstrated that the introduction of temporary electron-reservoir sites into the light-harvesting center greatly enhances the "quick recovery of photosensitization capability", which leads to improved photocatalytic efficiency in H_2 production from water. This certainly has much relevance for researchers established in the field of natural photosynthesis. Extended studies are still in progress in our laboratory.

Received: December 26, 2013
Published online: March 28, 2014

Keywords: artificial photosynthesis · hydrogen · photochemistry · pigments · platinum

[1] a) A. J. Esswein, D. G. Nocera, *Chem. Rev.* **2007**, *107*, 4022–4047; b) K. Sakai, H. Ozawa, *Coord. Chem. Rev.* **2007**, *251*, 2753–2766; c) L. Duan, F. Bozoglian, S. Mandal, B. Stewart, T. Privalov, A. Llobet, L. Sun, *Nat. Chem.* **2012**, *4*, 418–423; d) M. Wang, L. Chena, L. Sun, *Energy Environ. Sci.* **2012**, *5*, 6763–6778; e) D. J. Wasylenko, R. D. Palmer, C. P. Berlinguette, *Chem. Commun.* **2013**, *49*, 218–227; f) M. Wang, L. Chen, X. Li, L. Sun, *Dalton Trans.* **2011**, *40*, 12793–12800; g) S. Losse, J. G. Vos, S. Rau, *Coord. Chem. Rev.* **2010**, *254*, 2492–2504; h) V. Balzani, A. Credi, M. Venturi, *ChemSusChem* **2008**, *1*, 26–58.

[2] a) P. D. Tran, V. Artero, M. Fontcave, *Energy Environ. Sci.* **2010**, *3*, 727–747; b) S. Fukuzumi, Y. Yamada, T. Suenobu, K. Ohkubo, H. Kotani, *Energy Environ. Sci.* **2011**, *4*, 2754–2766; c) K. J. Young, L. A. Martini, R. L. Milot, R. C. Snoeberger III, V. S. Batista, C. A. Schmuttenmaer, R. H. Crabtree, G. W. Brudvig, *Coord. Chem. Rev.* **2013**, *256*, 2503–2520; d) J. H. Alstrum-Acevedo, M. K. Brennaman, T. J. Meyer, *Inorg. Chem.* **2005**, *44*, 6802–6827; e) D. Gust, T. A. Moore, A. L. Moore, *Acc. Chem. Res.* **2009**, *42*, 1890–1898.

[3] a) H. Ozawa, M. Haga, K. Sakai, *J. Am. Chem. Soc.* **2006**, *128*, 4926–4927; b) S. Masaoka, Y. Mukawa, K. Sakai, *Dalton Trans.* **2010**, *39*, 5868–5876; c) H. Ozawa, M. Kobayashi, B. Balan, S. Masaoka, K. Sakai, *Chem. Asian J.* **2010**, *5*, 1860–1869; d) H. Ozawa, K. Sakai, *Chem. Commun.* **2011**, *47*, 2227–2242; e) G. Ajayakumar, M. Kobayashi, S. Masaoka, K. Sakai, *Dalton Trans.* **2011**, *40*, 3955–3966; f) C. V. Suneesh, B. Balan, H. Ozawa, Y. Nakamura, T. Katayama, M. Muramatsu, Y. Nagasawa, H. Miyasaka, K. Sakai, *Phys. Chem. Chem. Phys.* **2014**, *16*, 1607–1616.

[4] R. Okazaki, S. Masaoka, K. Sakai, *Dalton Trans.* **2009**, 6127–6133.

[5] a) M. Kobayashi, S. Masaoka, K. Sakai, *Dalton Trans.* **2012**, *41*, 4903–4911; b) M. Kobayashi, S. Masaoka, K. Sakai, *Angew. Chem.* **2012**, *124*, 7549–7552; *Angew. Chem. Int. Ed.* **2012**, *51*, 7431–7434.

[6] a) A. Fihri, V. Artero, M. Razavet, C. Baffert, W. Leibl, M. Fontecave, *Angew. Chem.* **2008**, *120*, 574–577; *Angew. Chem. Int. Ed.* **2008**, *47*, 564–567; b) A. Fihri, V. Artero, A. Pereira, M. Fontecave, *Dalton Trans.* **2008**, 5567–5569.

[7] P. M. Gidney, R. D. Gillard, B. T. Heaton, *J. Chem. Soc. Dalton Trans.* **1973**, 132–134.

[8] M. Ogawa, G. Ajayakumar, S. Masaoka, H.-B. Kraatz, K. Sakai, *Chem. Eur. J.* **2011**, *17*, 1148–1162.

[9] M. Ogawa, B. Balan, G. Ajayakumar, S. Masaoka, H.-B. Kraatz, M. Muramatsu, S. Ito, Y. Nagasawa, H. Miyasaka, K. Sakai, *Dalton Trans.* **2010**, *39*, 4421–4434.

[10] a) C. Lee, C. Kim, M. S. Moon, J. W. Park, *Bull. Korean Chem. Soc.* **1994**, *15*, 909–911; b) C. Lee, Y. M. Lee, M. S. Moon, S. H. Park, J. W. Park, K. G. Kim, S.-J. Jeon, *J. Electroanal. Chem.* **1996**, *416*, 139–144; c) C. Lee, M. S. Moon, J. W. Park, *J. Electroanal. Chem.* **1996**, *407*, 161–167; d) J. W. Park, N. H. Choi, J. H. Kim, *J. Phys. Chem.* **1996**, *100*, 769–774.